Available online at www.sciencedirect.com

ScienceDirect

Ceramics International 35 (2009) 381–390

CERAMICS INTERNATIONAL

www.elsevier.com/locate/ceramint

Structural analysis on spinel ($MgAl_2O_4$) for application in spinel-bonded castables

A. Banerjee, S. Das, S. Misra, S. Mukhopadhyay *

Department of Chemical Technology, Calcutta University, 92 A.P.C. Road, Kolkata 700009, India

Received 10 June 2007; received in revised form 13 September 2007; accepted 12 November 2007
Available online 23 December 2007

Abstract

An intimate mixture of common hydrated magnesium salt and cheaper boehmite sol had been used as a cost-effective precursor of reactive nanometric spinel (1:1) powder. It was gelled at controlled pH, temperature and time, and calcined at significantly lower temperature after soft mechanochemical treatment. X-ray diffraction (XRD), infrared spectra, differential thermal analysis (with thermogravimetry), proton-nuclear magnetic resonance (NMR) and transmission electron microscope studies were carried out to investigate the incipient formation of low crystalline nanosized domains in the still-hydrated spinel. Spinel nanoparticles are protected by a thin chemisorbed layer of (OH) groups held around the active surface of the aggregates. Selected properties of conventional Al_2O_3–spinel and Al_2O_3–MgO castables were compared with the same formulated by the chemical-route spinel fines. Cold and hot strengths of the refractory castable containing commercial spinel with excess alumina powder were the best, while the same bonded by reactive magnesia and coprecipitated spinel fines were not satisfactory. Performance of sol–gel spinel is comparable to the preformed spinel with 78% alumina.

Keywords: Boehmite; Spinel; Refractory castable; Sol–gel

1. Introduction

In steel ladles, the performances of Al_2O_3–MgO and Al_2O_3–spinel castables have been investigated with profound interest in past few years. The important criteria leading to improvements of these castables are resistance towards high basic corrosive slags and their penetration, spalling resistance, drying behaviour and hot strength [1–5]. Both of these two varieties, although successful in application, have their demerits too, e.g. preformed spinels are expensive and entail multiple processing steps; in situ spinel also has some poor side effects like extensive hydration when MgO addition is beyond a certain limit. Incorporation of carbon into castables, in the form of Al_2O_3–MgO–C and Al_2O_3–SiC–C systems, has become an alternative approach in recent times [6,7]. However, carbon content in refractories is not environment friendly always, and cost factor related to stringent quality control may arise when 'micropelletized graphites' are used with antioxidants, coatings and binders [8]. A prospective route for preparing such unshaped refractories can be with nanocrystalline spinel synthesized by a modified sol–gel method [9,10]. The large negative free energies of formation of spinel, high melting point and wide range of its stoichiometry offer an important basis [11] towards the advantage of spinel from a fundamental perspective. In our previous work [10], it has been observed that such chemically prepared reactive spinel in castable might encounter the problems associated with the aggressive condition of steel ladles. It examined potentially useful strategies for the introduction of nanoscale microstructural features in spinel–alumina castables in a controlled manner. However there are still some unexplored sites and new findings in this area, which will be discussed in this work.

The field of nanostructured materials is widening nowadays in several directions. Chemistry has played a major role in the synthesis and modification of such materials. There is a tremendous interest and growing demand for the production of high quality ceramic nanopowders for various technological applications with specific scientific significance [12]. It is known that a reduction of material dimension in nanoscale, demonstrates substantial changes in physical, chemical and

---

* Corresponding author. Tel.: +91 33 2350 8386; fax: +91 33 23519755.
E-mail address: msunanda_cct@yahoo.co.in (S. Mukhopadhyay).

0272-8842/$34.00 © 2008 Elsevier Ltd and Techna Group S.r.l. All rights reserved.
doi:10.1016/j.ceramint.2007.11.009

mechanical properties. This paper is focused on investigation and development of reactive spinel-bonded high alumina castables and the requirement of production of stable spinel nanopowder by less cumbersome method.

As the chief precursor material was the boehmite sol, so the evolution of such gel network and subsequent thermal changes in it have been discussed elaborately in this paper. The work primarily attempts to ascertain the structural analogy of hydoxylated $MgAl_2O_4$ nanoparticle and its conversion from precursors by proton-nuclear magnetic resonance (NMR), FTIR, TEM, X-ray diffraction (XRD) and DTA/TG studies. An additional study documents the comparative performance of alumina-rich (R-type) spinel-bonded high alumina castable with that nanocrystalline counterpart, in terms of hot strength and physical properties. In situ Al_2O_3–MgO castable, coprecipitated spinel-bonded castable and P type (78% Al_2O_3) spinel-bonded castables were also considered for this investigation.

2. Experimental

The spinel hydrogel, as mentioned in our earlier work, put some adverse effects when used in castable batch beyond a certain amount. Due to this, the semidried gel precursors (G and C) were activated by 'soft' mechanochemical treatment [13] and optimally calcined at 900 °C. Modified in situ spinel additives were thus prepared after passing them through 200-mesh BS (below 75 μm) sieve. These fine materials (Table 1) were considered to be the important constituents of the respective matrices of the castable batches (Table 2). Two commercial preformed spinel powders (P and R) were collected from the market (Table 3) to incorporate into the new castable batch. All such powders had been utilized one at a time separately in equal amount (i.e. 8.0 wt%). Light and pure MgO fine (code M, Table 4) was also added to that batch (Table 2) to prepare in situ spinel-bonded high alumina (i.e. MgO–Al_2O_3) castable.

The procedure for castable preparation (named RN, GN, PN, MN and CN in accordance with the additives used) included dry and wet mixing of the batch, both done for 30 min to enhance the consistency of the mix. The mass was then cast in moulds and tamped within a particular time period. The material being self-flow type, no vibration was applied from outside. Curing in humid condition (for 24 h), air-drying (24 h) and oven drying (at 110 °C for 3 days) were strictly followed for all the samples. Finally they were heat treated (@ 5–8 °C/min) to 900, 1200, 1500 and 1600 °C with a holding period of 2 h in each case. Cube (25.4 mm) and bar (150 mm × 25 mm × 25 mm) moulds were used to prepare and characterize all kinds of spinel-bonded castables studied in this work. A simulated matrix composition of spinel-free castable was also formulated in this work (Table 5). It is worthwhile to mention that the performance of RN type castable has not been reported in our previous two articles [10]. In this paper, therefore, the quality of RN castable has been examined distinctively in comparison with others especially in terms of hot strength and physical properties.

Table 1
Special features of chemically prepared (G and C type) modified spinel powders incorporated in the castable matrix

Characteristics	Sol–gel derived (G)	Coprecipitated (C)
Particle size (μm)	<75	<75
Crystalline phases fully appeared at (°C)	600	1000
Respective crystalline size (apparent)	18 nm	0.14 μm
Al_2O_3 (wt%)	71.5	73.3
MgO (wt%)	28.5	26.7
True-specific gravity	3.02	2.46

Table 2
High alumina-based castable batch containing spinel forming additive in the matrix

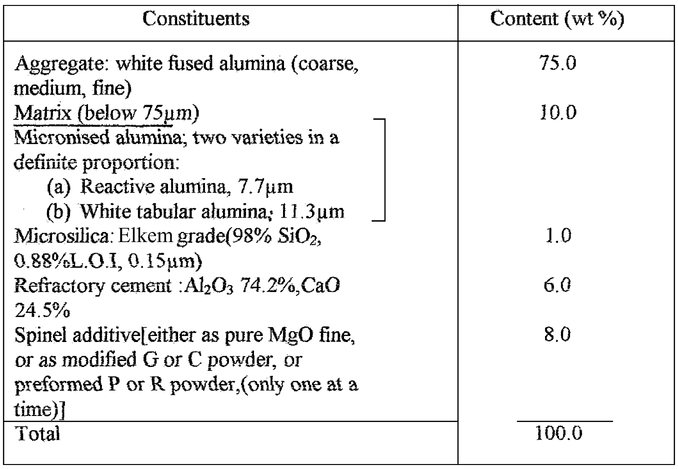

Constituents	Content (wt %)
Aggregate: white fused alumina (coarse, medium, fine)	75.0
Matrix (below 75μm) Micronised alumina; two varieties in a definite proportion: (a) Reactive alumina, 7.7μm (b) White tabular alumina, 11.3μm	10.0
Microsilica: Elkem grade(98% SiO_2, 0.88%L.O.I, 0.15μm)	1.0
Refractory cement :Al_2O_3 74.2%,CaO 24.5%	6.0
Spinel additive[either as pure MgO fine, or as modified G or C powder, or preformed P or R powder,(only one at a time)]	8.0
Total	100.0

Table 3
Characteristics of preformed magnesium-aluminate fines

Characteristics	P-type spinel	R-type spinel
Major constituents (wt%)		
Al_2O_3	>77.0	>90.0
MgO	>22.0	>8.9
True specific gravity	3.58	3.74
Particle size (μm)	Below 45	Below 45

Table 4
Characteristics of light chemical grade magnesia powder

MgO (wt%)	92.4
Crystal phase	Periclase
True-specific gravity	3.30
Average particle size (μm)	20.0
Surface area (m^2/g)	10.3
SiO_2 (wt%)	0.12
CaO (wt%)	0.42
B_2O_3 (wt%)	0.005
Al_2O_3 (wt%)	0.04
Fe_2O_3 (wt%)	0.03
Percent loss of ignition (including chloride, hydroxyl, carbonate and sulphate)	7.0 (approximately)

Table 5
Matrix composition of spinel-free castable

Constituents	Amount (wt%)
Micronised alumina	58.80
High alumina/refractory cement	35.30
Microsilica	5.90
Total	100.0

Proton-NMR studies of the dried boehmite gel and nanometric spinel powder were carried out by Bruker AV 300 Supercon NMR spectrometer using deuterated chloroform, $CdCl_3$, as the solvent. Differential thermal analysis and thermogravimetry (DTA and TGA) were done in air atmosphere at a rate 10 K/min (in air) by an instrument NETZSCH thermal analyzer (model: STA 409 C). The infrared spectral pattern (IR) was taken from an instrument JASCO, FT/IR-670 Plus (Japan) following the KBr method. Cold crushing strength (CCS), apparent porosity (A.P.) and bulk density (B.D.) of all the castables were performed by standard ASTM methods. An average of four samples was considered for all such tests. The HMOR study (1400 °C) of all five types of specimens were carried out by the conventional three-point bending method with the bar type samples. The X-ray diffraction phase analysis of the heat-treated castable samples was performed using a 'Philips Analytical' instrument with Ni-filtered Cu Kα radiation. The thermal shock resistance (spalling) test was carried out by the well known water-quenching method (from 800 °C to cold water) and then determining the residual CCS (i.e. %RS) values of the cubes, retained after five such cycles. The TEM study using the finer fraction of the G type calcined (900 and 1500 °C) powder was performed to verify the existence of nano-dimensional spinel crystallites in it. It was the same Hitachi H-600 (bright field, 50 kV) model used in our last work. This was also utilized to study the TEM patterns of 'R' type preformed spinel powder and 'C' type chemically prepared powder.

3. Results and discussion

The spinel gel has been prepared from water compatible and inexpensive boehmite sol by adding a magnesium salt to it. The stable boehmite sol has been synthesized from nitrate precursor [14]. Therefore the ease of conversion of spinel may be better understood by the XRD pattern of boehmite after calcination at different temperatures (Fig. 1a). The XRD peaks at 200, 500 and 800 °C strongly suggest the conversion of boehmite (γ-AlOOH) to γ-Al_2O_3. The tiny domains of boehmite crystallites as indicated by the broad XRD pattern at 200 °C might yield reactive γ-Al_2O_3. It has been reported that residual water is adsorbed on the surfaces of nanocrystalline boehmite particles [15,16], because of a newly formed large amount of surfaces [17]. It is also known that heating boehmite in air above 400 °C produces a fine, lamellar, porous microstructure that is reorganized to result in the spinel structure of γ-Al_2O_3 [18,19]. The porosity of the product can be controlled by the partial pressure of water, and the interlamellar gap depends on the free energy associated to the formation of new surface during dehydration. So there might be an orientational correlation between the starting material (boehmite gel) and the final product (magnesium-aluminate spinel) via the intermediate structure of γ-Al_2O_3 phase [20]. Cubic γ-Al_2O_3 can be regarded as defective normal spinel (AB_2O_4) if its formula were expressed as $Al_{2.67}O_4$ [21], where two Al^{3+} ions are accommodated to the octahedral voids while $0.67Al^{3+}$ ions to tetrahedral voids. Consequently faster and earlier incipient hydrated spinel formation via topochemically transformed γ-Al_2O_3 could be possible, if a controlled heating is applied to the boehmite sol mixed with Mg-salt. In that case the reactive seeds of MgO and γ-Al_2O_3 produces spinel phase at as low as 450 °C with a significant saving of energy [22]. A mechanochemical activation of the combined gel mass with one hydroxide component might facilitate this transformation [23–25].

It is known that the γ-AlOOH precursor exists as the unhydrolyzed species $[Al(H_2O)_6]^{3+}$ below a certain pH. That aqua ion or a deprotonated ion can exist stably and they can be polymerized at controlled pH, through the formation of 'Keggin' type tridecamer cluster [26]. Here a central AlO_4 tetrahedron is surrounded by 12 numbers of AlO_6 octahedrons with perfect tetrahedral symmetry and the acid/Al ratio determines the degree of compactness of the network [27]. When treated to a temperature of 800 °C, Al in such material is known to be present in a variety of coordinated sites with oxygen vacancy [28]. It has also been reported that, during spinel preparation [24] grinding may cause a change in bond status. If some of the octahedral Al of hydroxylated alumina in boehmite could be partly converted to tetrahedral coordination, the formation of γ-Al_2O_3 might be expected in the next step quite earlier. Since the intermediate product (γ-Al_2O_3) contains both tetrahedral and octahedral aluminium with incipient spinel character, the evolution of a parental material closer to γ-Al_2O_3 prior to complete thermal dehydration will be obviously beneficial. Due to this reason soft mechanochemical treatment was applied before the calcination of spinel hydrogel.

The DTA/TGA report (Fig. 1b) of boehmite gel confirms stepwise changes observed with increasing temperature. Major weight losses occur due possibly to the volatilization of water and decomposition of nitrates and minor losses between 600 and 1200 °C [29]. Accordingly, the main weight losses at 122, 240 and 329 °C may be due to the loss of free water, elimination of bonded water, decomposition of some adherent NH_4NO_3 in gel and conversion of boehmite to γ-Al_2O_3 phase. However the dehydration goes up to 900 °C and above, might be due to the release of residual hydroxyl groups attached to the reactive surfaces of the material. The formation of boehmite to γ-Al_2O_3 before 500 °C has already been seen in the XRD report [17]. The conversion to α-Al_2O_3 beyond 1100 °C is also clear from the DTA trace.

The proton-NMR report (Fig. 1c) of the dried boehmite gel (200 °C) supports the existence of remnant (OH) groups. The small peak near by 2.3 ppm is possibly associated with the protons of structural Al–OH groups [30]. The other peak at 1.57 ppm also indicates the presence of OH-groups. It is also known that more hydrogen is observed sometimes than

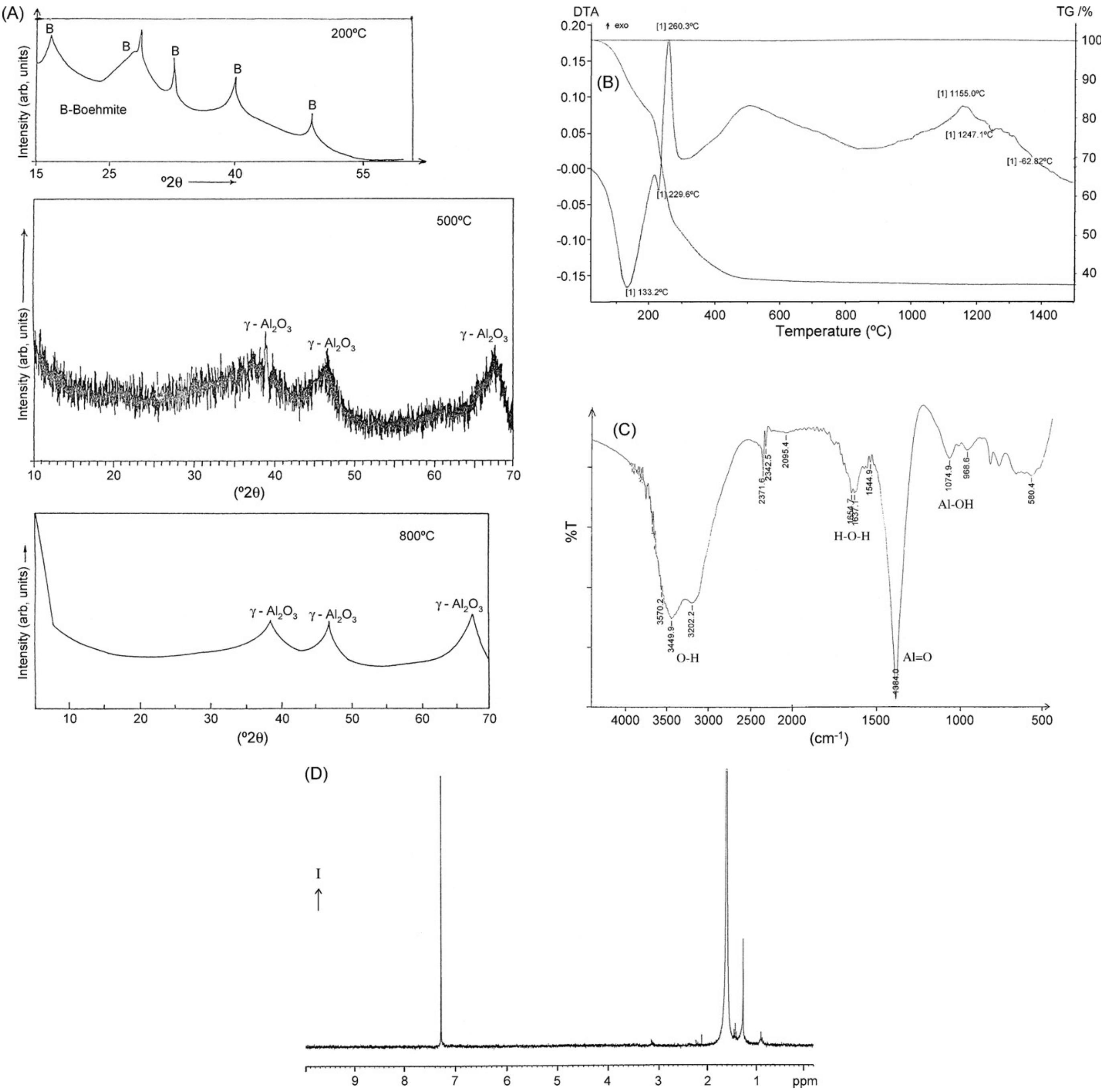

Fig. 1. (a) XRD phase evolution of boehmite with increasing temperature; (b) DTA and TGA traces of boehmite gel; (c) FTIR spectral pattern of dried boehmite gel; (d) proton-NMR pattern of dried boehmite gel.

indicated by LOI experiments and significantly higher surface area than typically expected for crystalline boehmite derived γ-alumina, is present due to nanopores [31]. Those authors considered one protospinel structure ($Al_2O_3 \cdot 0.2H_2O$) with one (OH) per unit cell and showed that the molecular water in gel-derived alumina decreases with increasing temperature up to 800 °C. In our work, however, we already reported the existence of residual water layer till 900 °C in the magnesium-aluminate spinel [9].

Fig. 1d represents the IR spectra of dried boehmite. Al–OH stretching is observed at 3297 and 3050 cm^{-1} along with a sharp O–H stretch at 3671 cm^{-1}. H–O–H bend is at 1630 (free water) and at 3500 cm^{-1}. Al–OH bending is observed at 1070 and 1160 cm^{-1} while Al–O vibration is nearby 950 cm^{-1} [32,33].

The precursor powder has been prepared by a modified sol–gel route. In this regard, firstly the boehmite sol has been stabilized in the acidic pH range. The spinel hydrosol was prepared thereafter by controlling the temperature, pH, stirring rate of the mix during the careful addition of Mg-salt. In the hydrosol of spinel, a charged double layer surrounding nanoparticles produce a coulombic barrier to aggregation that

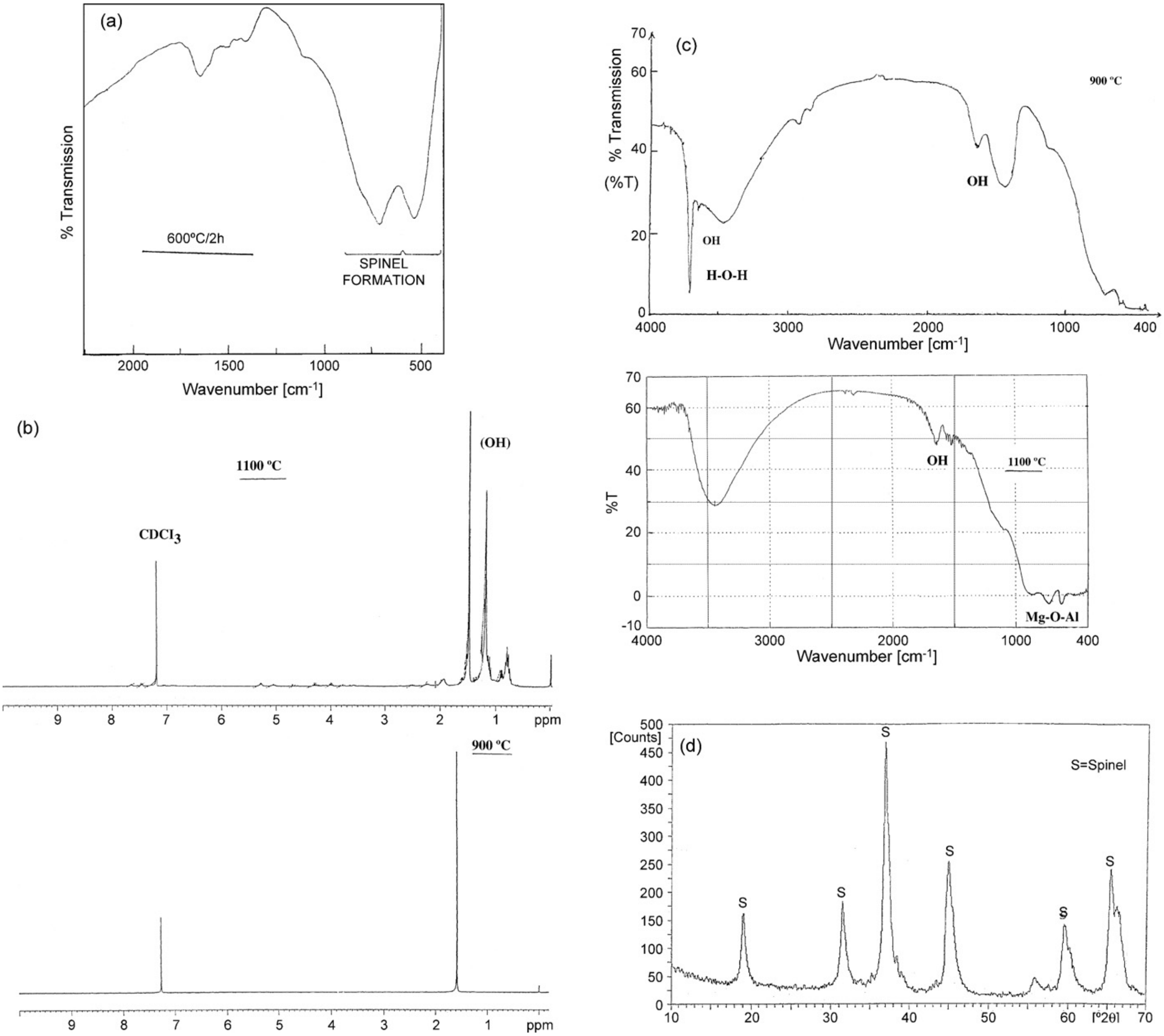

Fig. 2. (a) IR pattern of hydrated spinel ($MgAl_2O_4$) precursor calcined at 600 °C; (b) proton-NMR reports of spinel additive calcined at 900 and 1100 °C; (c) IR patterns of the spinel additive calcined at 900 and 1100 °C; (d) XRD trace of the spinel powder calcined at 1100 °C.

stabilizes the colloidal entities. It is known that nanomaterials are secured by some capping agents, which control their high reactivity and determine the size of nanoaggregates. It is also known that there are many hydrated salts of Al^{3+} and Mg^{2+}, which hydrolyze at elevated temperature by its own water of crystallization, and cannot be made completely anhydrous by heating alone up to a reasonable temperature. It is suggested here that the hydrogel of spinel ($MgAl_2O_4{\cdot}xH_2O$, $x < 1$) retains similar feature, and the (OH) groups surrounding the unit cell aggregates of spinel, behave as capping agent of the required nanoparticle as well as a reducing agent. The reactive precursor is therefore, primarily important to derive the spinel phase at lower temperature via modified sol–gel route. Secondly the stoichiometry of $MgAl_2O_4$ (1:1) can be precisely maintained and tailor made oxide composition may be prepared from such precursor. The TEM of such powder, as shown later also supports the preservation of nanoparticles in the material.

The sol–gel route is always advantageous to get complete spinel phase at a significantly lower temperature, e.g. 600 °C [10]. Fig. 2a is the IR pattern of that powder showing the strong Mg–O–Al linkage at 525–690 cm^{-1}, however a lot of residual hydroxyl groups are associated with its structure. As mentioned before, the calcined gel material retains some active sites and helps forming weak chemical bonds. It appears that liquid (water) molecules have easily been chemisorbed over the solid surfaces. The NMR report (Fig. 2b and c) of the spinel additive also indicate that the precursor structure contains some remnant (OH) groups even above 900 °C; when heated beyond 1100 °C, they must create some pores or active sites till available for chemisorption of water. The IR pattern (Fig. 2d) of the

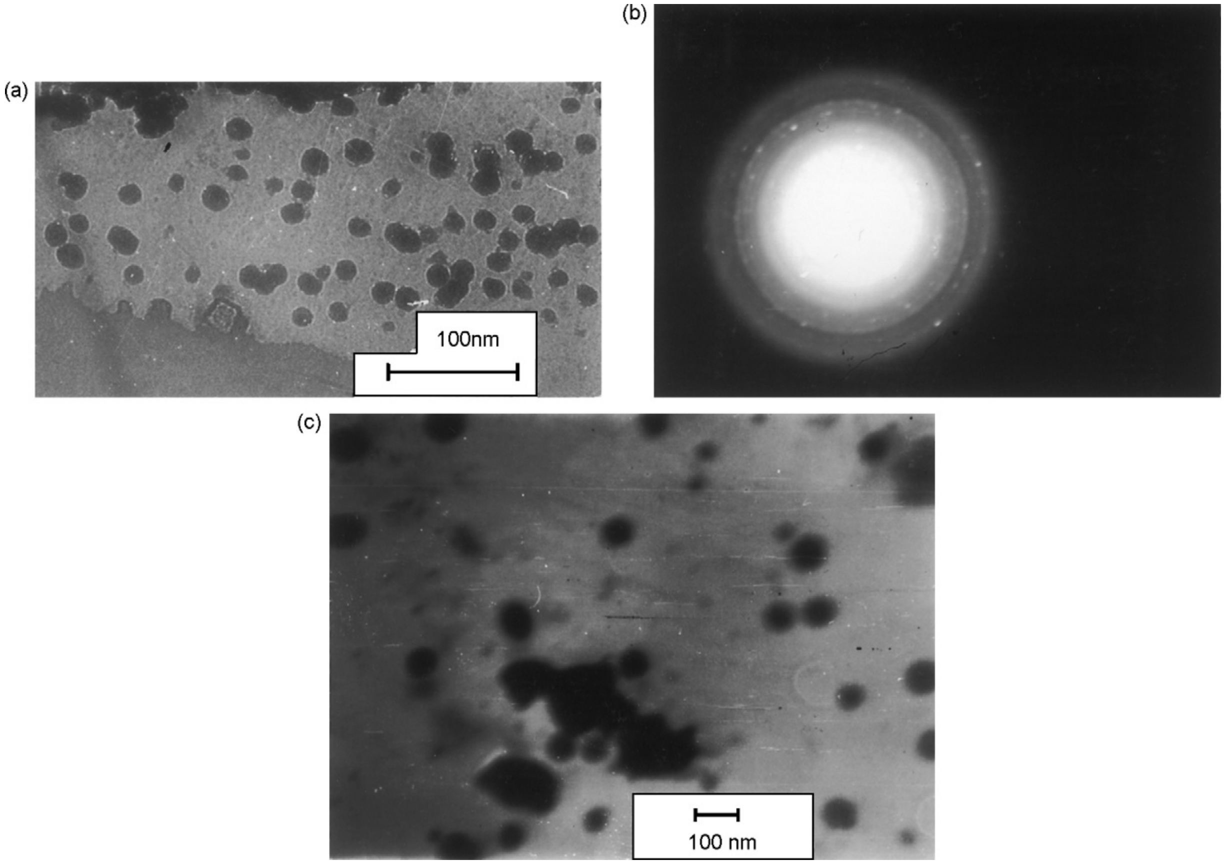

Fig. 3. (a) TEM micrograph of spinel additive calcined at 900 °C with (b) SAED pattern, and (c) TEM micrograph of spinel additive calcined at 1500 °C.

precursor powder calcined at 900 °C indicates the existence of residual hydroxyl groups present within the structure. The peaks nearby 3500 cm^{-1} indicate that the structure must have been associated with some residual hydroxyl groups. As discussed later, when the castable cubes containing such spinel powders are fired beyond 1200 °C, these hydroxyl groups help to form some finer nanopores in the refractory. Even the powder calcined at 1100 °C (Fig. 2e), entangles some residual moisture as also clear from the relevant H NMR report. Chemisorption here could be recognized as the formation of a chemical bond after the rearrangement of electron density in water (adsorbate) and the spinel (substrate). As such the status of such bonds lie anywhere between the complete ionic or covalent bonds, and removal of chemisorbed species from the active sites of surface is possible under extreme condition such as high temperature treatment. The activation energy, i.e. the enthalpy of adsorption related to the strength of such chemisorbed bond, would possess nearly the same order of magnitude as the energy change in a chemical reaction [34,35].

Crystallization of spinel gel at very low temperature indicates that the precursor has small reactive clusters with appropriate chemical homogeneity. During heat treatment respective metal oxides are produced in nascent states; these are basically tiny atomic clusters with correct chemical homogeneity embedded in a mesoporous network. These nascent metal oxides react very fast to form the desired single phase of $MgAl_2O_4$. Evolution of water vapour causes the agglomerated particles to decompose that inhibits further the growth of nanosized particles by sintering [36]. The precursor powder, already mentioned, retains a chemisorbed monolayer having some (OH) groups entangled with the structure although the spinel crystallites have been developed prominently. The XRD trace of the material fired at 1100 °C (Fig. 2f) shows moderately broadened peaks that infer the presence of fine crystallites of spinel in the still-hydrated material. The ratio of intensity of (3 1 1) and (4 0 0) reflections confirm the complete evolution of cubic spinel. The novel sol–gel route assisted with mechanical treatment thereby stands more useful than both pure solid-state reaction and pure wet chemistry based synthesis.

The TEM micrographs of modified spinel additive (Fig. 3a and b) calcined at 900 °C clearly shows that nanoparticles are present in it. The same additive, when treated to 1500 °C and ground, some fraction till preserves the nano-dimension (Fig. 3c). Such OH-induced nanostructural build up of spinel particles may be utilized to activate and modify the surface for a specific application. In this work with high alumina castable, it has been intended to use this nanofine additive to get a two-fold benefit out of it, which will be discussed later.

Unlike those TEM micrographs, the TEM pattern of 'R' additive (Fig. 4a) shows that the particles present here are in micron ranges. As the synthesis temperature of such preformed additive is too high (∼2000 °C) and as the manufacturing process involves so many stipulated steps, namely precalcination, grinding, granulation, sintering, etc., chances are

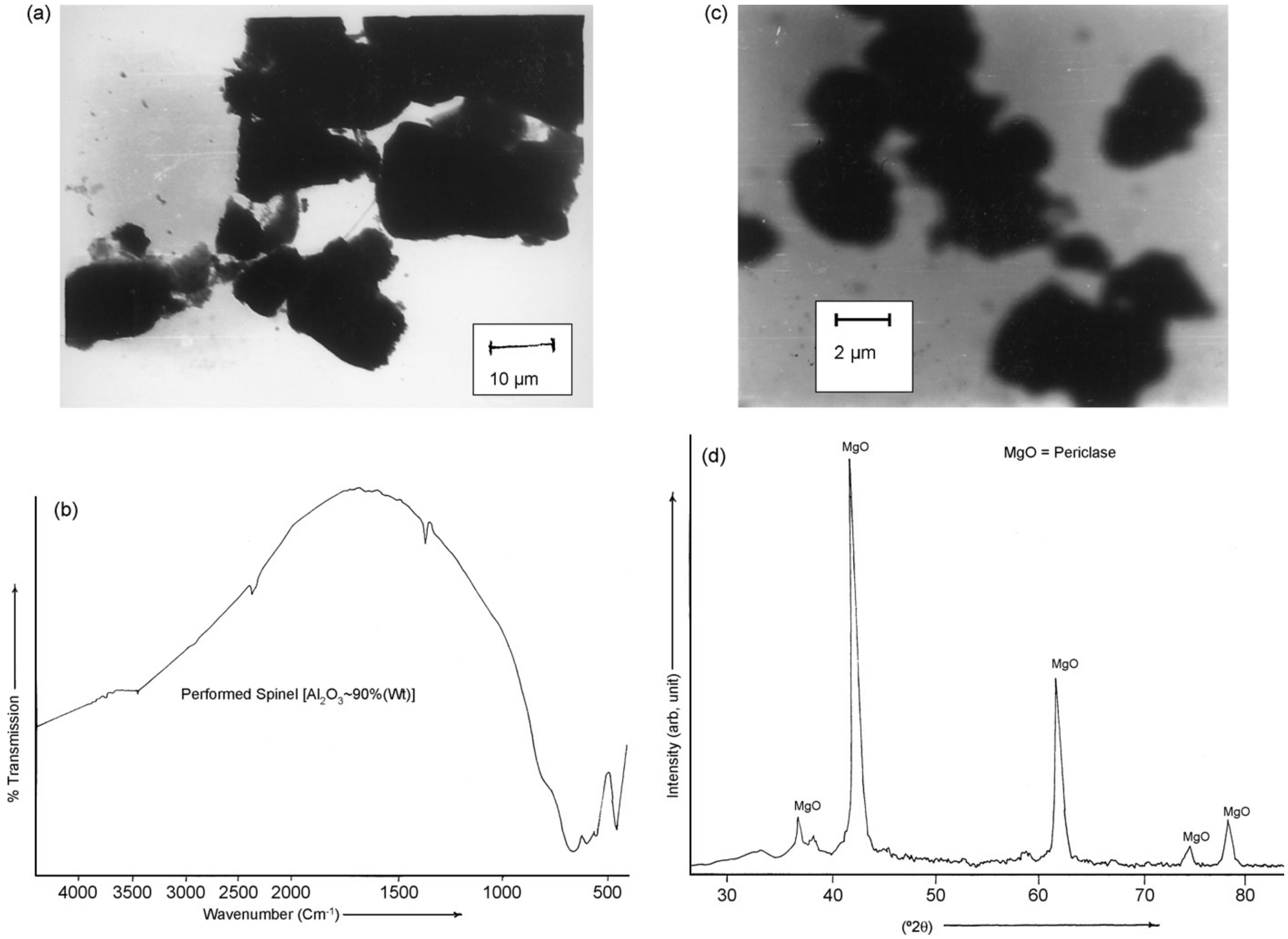

Fig. 4. (a) TEM micrograph of R type alumina-rich preformed spinel powder; (b) IR pattern of R type alumina-rich preformed commercial spinel powder; (c) TEM micrograph of C type coprecipitated spinel fine calcined at 1500 °C; (d) XRD pattern of MgO additive (code M) utilized to prepare in situ castable.

obviously less to retain nanosizes of the particles. However, a major advantage of such commercial ‘R’ type spinel is that it is enriched with corundum phases. As found in literature [37], the alumina content established from the lattice constant of some spinel by XRD, may not always comply with that given in specification. Actually the MgO–Al_2O_3 phase diagram indicates that spinel forms a solid solution at high temperature with excess of both Al_2O_3 and MgO; however these non-stoichiometric solid solutions are metastable at room temperature so that the cooling rate from sintering or fusion temperature is an important factor for preparing preformed spinels. As a consequence, some commercial spinels contain some secondary phases, as we see for ‘R’ type here. The excess alumina here, remains as free corundum fines. It is substantiated by the IR pattern (Fig. 4b), where a small peak at ~1345 cm^{-1} and larger one at ~450 cm^{-1} might possibly arise due to Al=O linkage of free Al_2O_3, whereas the adjacent spinel forming peaks are located around 600 cm^{-1}. The ‘C’ type additive (Fig. 4c) also shows the agglomerated particles in its TEM micrograph.

The other features of P type spinel and modified coprecipitated spinel (‘C’ type) have been stated in our earlier publications [9,10]. The batch composition of five type of spinel-bonded castables (RN, GN, PN, CN, MN) has been given in Table 2. Out of them, the first four may be categorized as Al_2O_3–spinel castable. The ‘MN’ type belongs to in situ Al_2O_3–MgO castable, where, in place of spinel, an equal amount of LR grade light, magnesia fines has been added. The XRD pattern of MgO additive (Fig. 4d) shows strong peaks of periclase phase.

Fig. 5a shows the XRD pattern of matrix part of spinel-free castable (Table 5) heated to 900 °C, which confirms the CA and CA_2 phases [C=CaO, A=Al_2O_3] with corundum. Actually the dehydration of cementitious phase gave rise to such phases, which is the root cause of increase in porosity and fall in BD of castables at the intermediate temperature range. Due to this prevailing feature, a break is very much conspicuous in ‘A.P.’ and ‘CCS’ curves (Fig. 5b and c) of all five castables at 900 °C. Among all five samples (Fig. 5b and c), obviously the physical properties of ‘RN’ type castable are the best, whereas those of ‘PN’ and ‘GN’ are comparable. The spalling resistance of GN is, however, better than both PN (56%) and RN (51%), as reported elsewhere, due to the submicronised pores and microcracks present in its structure [10]. The XRD reports of GN, MN had also been described [10]. XRD reports of ‘RN’

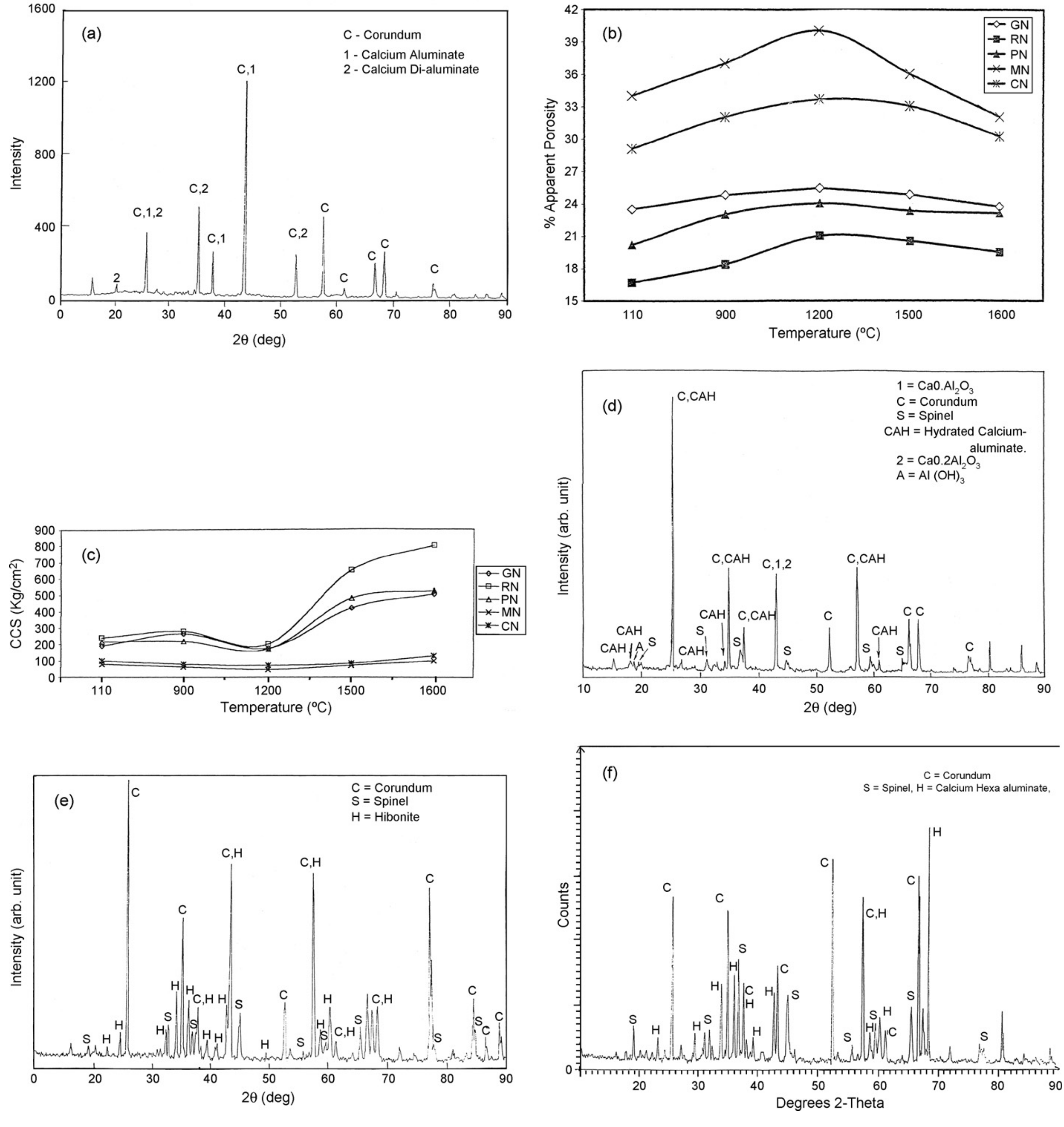

Fig. 5. (a) XRD pattern of matrix part of spinel-free castable heated at 900 °C/2 h; (b) variation of apparent porosity (A.P.) of five type castables (RN, GN, PN, MN, CN) with increasing temperature; (c) variation of cold crushing strength (CCS) of five type castables (RN, GN, PN, MN, CN) with increasing temperature; (d) XRD pattern of RN type castable dried at 110 °C/2 h; (e) XRD pattern of RN castable fired at 1600 °C/2 h; (f) XRD pattern of PN type castable fired at 1600 °C/2 h.

type castable (Fig. 5d and e) after heating at 110 and 1600 °C have been shown here. There is an abundance of reactive corundum fines in the 'RN' type, for which possibly excess gel of hydrated alumina is formed that raises the green strength of 'RN'. Such excess alumina fines also help to improve sintering and to yield an excessive amount of CA_6 phase at 1600 °C, which builds up a 3-dimensional network with spinels present in the matrix. This not only leads to a maximization of CCS and minimization of A.P. values, but also results in exceedingly well HMOR value (Table 6) of RN castable among those five [38,39]. The other two castables, MN and CN, exhibit no such interesting behaviour in terms of hot strength and physical properties, although the slag resistance of MN is remarkable. The XRD of PN castable (Fig. 5f) at 1600 °C shows that, it has

Table 6
HMOR of spinel-free and other five type castables

Type	HMOR (MPa)
Spinel-free	6.5
RN	13.7
GN	12.2
PN	12.8
MN	5.2
CN	7.4

some resemblance with RN type. However the absence of excess corundum fines restricts its properties with respect to RN. The properties of GN castable are very much promising, possibly due to some amount of nanoparticles present in the green batch, and due to the entrapment of nanopores and sporadic nano-dimensional structures retained in GN after heat treatment. This would become clear from atomic force microscopy (AFM), SEM and slag resistance studies discussed in our next publication.

4. Conclusions

From this laboratory scale investigation, the following conclusions may be drawn:

(1) Spinel nanoparticles can be prepared by boehmite sol as the chief precursor; with magnesium salt intimately mixed to it and heat-treated. The γ-Al_2O_3, with incipient spinel character, is an important intermediate in this preparation.
(2) A thin residual (OH) layer retained on the active surface of the spinel powder behaves as a capping agent of the nanoparticles. The spinel powder calcined at relatively mild condition (900 °C) assisted with soft mechanochemistry, can be an additive in spinel–alumina castable, for comparison with P type commercial spinel.
(3) R type preformed spinel, being enriched with excess corundum fines build up a strong CA_6-spinel–corundum linkage to exhibit the highest HMOR at par with other relevant properties. Coprecipitated spinel, in this work, failed to draw any considerable attention. In situ spinel–alumina castable could not escape the limitation of extensive hydration and volume expansion.

Acknowledgement

The authors gratefully acknowledge Prof. A. Patra, Department of Chemistry, Calcutta University, for his help extended during the course of this investigation.

References

[1] Y.C. Ko, Influence of the characteristics of spinels on the slag resistance of Al_2O_3–MgO and Al_2O_3–spinel castables, J. Am. Ceram. Soc. 83 (9) (2000) 2333–2335.
[2] P. Korgul, P.R. Wilson, W.E. Lee, Microstructural analysis of corroded alumina–spinel castable refractories, J. Eur. Ceram. Soc. 17 (1997) 77–84.
[3] F. Simonin, C. Olagnon, S. Maximilien, G. Fantozzi, Thermomechanical behaviour of high alumina refractory castables with synthetic spinel addition, J. Am. Ceram. Soc. 83 (2000) 2481–2490.
[4] M. Fuhrer, A. Hey, W.E. Lee, Microstructural evolution in self-forming spinel/calcium bonded refractories, J. Eur. Ceram. Soc. 18 (1998) 813–820.
[5] N. Schmitt, et al., Damage of monolithic refractory linings in steel ladles during drying, Br. Ceram. Trans. 103 (3) (2004) 121–133.
[6] S. Palco, N. Zhou, M. Rigaud, Al_2O_3–MgO–C castables for steelmaking ladles: recent developments and improvements, in: Electric Furnace Conference Proceedings, 2000, p. 433.
[7] T. Kaji, Y. Ono, T. Ishino, Development of carbon containing castables for iron and steel making, in: 9th UNITECR-2005, 8–11th November, Orlando, Florida, USA, 2005.
[8] S. Zhang, W.E. Lee, Carbon containing castables: current status and future prospects, Br. Ceram. Trans 101 (1) (2002) 1–8.
[9] S. Ghosh, R. Lodha, P. Barick, S. Mukhopadhyay, Improvement of thermal characteristics of refractory castable by addition of gel-route spinel nanoparticle, Mater. Manuf. Process. 22 (2007) 81–90.
[10] (a) S. Mukhopadhyay, et al., Influence of gel-derived nanocrystalline spinel in a high alumina castable: Part 1, Ceram. Int. 31 (2) (2005) 333–347;
(b) S. Mukhopadhyay, et al., Influence of gel-derived nanocrystalline spinel in a high alumina castable: Part 2, Ceram. Int. 33 (2) (2007) 175–186.
[11] R.C. Bradt, Mg–Al spinel: is it the mullite of the 21st century? RA News 9 (4) (2004) 8–9.
[12] (a) B.K. Panda, B.B. Sahu, V. Rajendran, N. Suresh Kumar, K. Jeyasubramanium, Preparation and characterization of nanosized TiO_2 powder for refractory applications, in: Proceedings of Eighth International Conference on Nanostructured Materials (NANO-2006), Indian Institute of Science, Bangalore, India, August 20–25, (2006), p. 150;
(b) A. Beitollahi, S.A.M. Haghgo, Synthesis and characterization of ceria nanopowders by solution combustion method, in: Proceedings of Eighth International Conference on Nanostructured Materials (NANO-2006), Indian Institute of Science, Bangalore, India, August 20–25, (2006), p. 89;
(c) S. Mathur, C. Cavelius, Molecular chemical concepts for solvothermal growth of oxide nanostructures, in: Proceedings of Eighth International Conference on Nanostructured Materials (NANO-2006), Indian Institute of Science, Bangalore, India, August 20–25, (2006), p. 161;
(c) T.P. Yadav, N.K. Mukhopadhyay, R.S. Tiwan, O.N. Srivastava, Synthesis and characterization of nanocrystalline (Ni,Fe)Al_2O_4 spinel powder by mechanical milling, in: Proceedings of Eighth International Conference on Nanostructured Materials (NANO-2006), Indian Institute of Science, Bangalore, India, August 20–25, (2006), p. 63.
[13] (a) Evgeny G. Avvakumov, Chem. Sustain. Dev. 2–3 (1994) 475;
(b) W.T. Bakker, J.T. Lindsay, Reactive magnesia spinel, preparation and properties, Am. Ceram. Soc. Bull. 46 (11) (1967) 1094–1097.
[14] P.de S. Santos, R.de F. Neves, H.de S. Santos, Preparation of aqueous sols containing well-shaped boehmite crystals, Colloid Polym. Sci. 271 (2) (1993) 197–200.
[15] (a) Y. Arai (Ed.), Chemistry of Powder Production, Chapman and Hall, N. York, 1996, , pp. 48–50, pp. 69–71;
(b) J.S. Reed (Ed.), Introduction to the Principle of Ceramic Processing, John Wiley and sons, New York, 1988, pp. 127–128.
[16] K. Itatani, A. Naitou, I.J. Davies, S. Sano, S. Koda, Formation process of magnesium aluminate due to solid-state reaction of highly dispersed and nanometer-sized particles, J. Soc. Inorg. Mater. Jpn. 13 (2006) 336–344.
[17] C.C. Yong, J. Wang, Mechanical-activation-triggered gibbsite-to-boehmite transition and activation-derived alumina powders, J. Am. Ceram. Soc. 84 (6) (2001) 1225–1230.
[18] S.J. Wilson, The dehydration of boehmite, γ-AlOOH to γ-Al_2O_3, J. Solid State Chem. 30 (1979) 247–255.
[19] S.J. Wilson, J.D.C. McConnell, M.H. Stacey, Energetics of formation of lamella or porous microstructures in γ-Al_2O_3, J. Mater. Sci. 15 (1980) 3081–3090.
[20] C.N.R. Rao, Topochemical reactions, in: Chemical Approaches to the Synthesis of Inorganic Materials, Wiley Eastern Ltd. (New Age Intl. Ltd.), New Delhi, 1994, pp. 31 (Chapter 6).

[21] D. Domanski, G. Urretavizcaya, F.J. Castro, F.C. Gennari, Mechanochemical synthesis of magnesium aluminate spinel powder at room temperature, J. Am. Ceram. Soc. 87 (11) (2004) 2020–2024.

[22] S. Mukhopadhyay, S. Ghosh, M.K. Mahapatra, R. Majumdar, P. Barick, S. Gupta, S. Chakraborty, Easy-to-use mullite and spinel sols as bonding agents in a high alumina based ultra low cement castable, Ceram. Int. 28 (7) (2002) 719–729.

[23] B.P. Singerova, N. Stevulova, M. Luxova, E.B. Zarova, Mechanochemical synthesis of magnesium aluminate spinel in oxide-hydroxide systems, J. Mater. Synth. Process. 8 (5–6) (2000) 287–293.

[24] K.J.D. Mackenjie, J. Temuujin, T.S. Jadambaa, M.E. Smith, P. Angerer, Mechanochemical synthesis and sintering behaviour of magnesium aluminate spinel, J. Mater. Sci. 35 (2000) 5529–5535.

[25] G. Ye, T. Troczynski, Mechanical activation of heterogeneous sol gel precursors for synthesis of $MgAl_2O_4$ spinel, J. Am. Ceram. Soc. 88 (10) (2005) 2970–2974.

[26] S. Sakka (Ed.), Handbook of Sol Gel Science and Technology: Processing, Characterization and Application, vol II, Sol Gel Processing, H. Kozuka (volume editor), Kluwer Academic Publishers, Boston, 2005, pp. 106 (Chapter 5).

[27] G. Fu, L.F. Nazar, A.D. Bain, Aging processes of alumina sol–gels: characterisation of new aluminium polyoxycations by 27Al NMR spectroscopy, Chem. Mater. 3 (1991) 602–610.

[28] Y. Kurokawa, T. Suga, S. Nakata, T. Ikoma, S.T. Kubota, Transparent alumina films derived from two sources of $AlCl_3\cdot6H_2O$ and aluminium isopropoxide by sol–gel method, J. Mater. Sci. Lett. 17 (1998) 275.

[29] M.K. Naskar, M. Chatterjee, Boehmite nanoparticles by the two-reverse emulsion technique, J. Am. Ceram. Soc. 88 (12) (2005) 3322–3326.

[30] J.J. Fitzgerald, G. Piedra, S.F. Dec, M. Segar, G.E. Maciel, Dehydration studies of a high-surface-area alumina (pseudo-boehmite) using solid state 1H and 27Al-NMR, J. Am. Chem. Soc. 119 (33) (1997) 7832–7842.

[31] G. Paglia, C.E. Buckley, T.J. Udovic, A.L. Rohl, F. Zones, C.F. Maitland, J. Connolly, Boehmite-derived γ-alumina system. 2: Consideration of hydrogen and surface effects, Chem. Mater. 16 (10) (2004) 1914–1923.

[32] E. Drabarek, K.S. Finnie, J.R. Bartlett, J.L. Woolfrey, D. Mitchell, Sol gel preparation of thick α-Al_2O_3 films on stainless steel, in: L.C. Klein, E.J.A. Pope, S. Sakka, J.L. Woolfrey (Eds.), Sol Gel Processing of Advanced Materials, The American Ceramic Society, Westerville (Ohio), Ceramic Transactions, vol. 81, 1998, pp. 119–132.

[33] M. Sathiyakumar, F.D. Gnanam, Synthesis of sol–gel derived alumina powder: effect of milling and calcinations temperatures on sintering behaviour, Br. Ceram. Trans. 98 (1999) 87–92.

[34] Chemisorption and catalysis, A.W. Adamson (Ed.), Physical Chemistry of Surfaces, fifth ed., John Wiley & Sons Inc., New York, 1990, pp. 682–745 (Chapter XVII).

[35] The properties of surfaces, P.W. Atkins (Ed.), Physical Chemistry, fifth ed., Oxford University Press, Oxford, 1994 , pp. 961–1006 (Chapter 28).

[36] M.F.M. Zawrah, A.A.El. Kheshen, Synthesis and characterization of nanocrystalline $MgAl_2O_4$ ceramic powders by use of molten salts, Br. Ceram. Trans. 101 (2) (2002) 71–74.

[37] C.F. Chan, Y.C. Ko, A study of commercial magnesia-alumina spinels for alumina-spinel castables, Interceram 47 (1998) 374–378.

[38] C.F. Chan, Y.C. Ko, Effect of CaO content on the hot strength of alumina-spinel castables in the temperature range of 1000 to 1500 °C, J. Am. Ceram. Soc. 81 (11) (1998) 2957–2960.

[39] Y.C. Ko, C.F. Chan, Effect of spinel content on hot strength of alumina-spinel castables in the temperature range of 1500 °C, J. Eur. Ceram. Soc. 19 (1999) 2633–2639.